Journal of Achievements in Materials and Manufacturing Engineering
VOLUME 29
ISSUE 2
August
2008

Thermal characteristics of the AM50 magnesium alloy

W. Kasprzak [a,c,*], J.H. Sokolowski [b], M. Sahoo [a], L.A. Dobrzański [c]
[a] Materials Technology Laboratory, 568 Booth Street,
Ottawa, Ontario, K1A 0G1, Canada
[b] Light Metals Casting Technology Group, University of Windsor,
401 Sunset Avenue, Windsor, Ontario, N9B 3P4, Canada
[c] Division of Materials Processing Technology, Management and Computer Techniques in Materials Science, Institute of Engineering Materials and Biomaterials,
Silesian University of Technology, ul. Konarskiego 18a, 44-100 Gliwice, Poland
* Corresponding author: E-mail address: wkasprza@nrcan.gc.ca

Received 12.04.2008; published in revised form 01.08.2008

Manufacturing and processing

ABSTRACT

Purpose: The goal of this publication is to demonstrate the laboratory metal casting simulation methodology based on controlled melting and solidification experiments. The thermal characteristics of the AM50 magnesium alloy during melting and solidification cycles were determined and correlated with the test samples' microstructural parameters.
Design/methodology/approach: A novel methodology allowed to perform variable solidification rates for stationary test samples. The experiments were performed using computer controlled induction heating and cooling sources using Ar for melt protection and test sample cooling.
Findings: Thermal analysis data indicated that the alloy's melting range was between approximately 434 and 640°C. Increasing the cooling rate from 1 to 4°C/s during solidification process reduced the Secondary Dendrite Arm Spacing from approximately 64 to 43μm. The temperatures of the metallurgical reactions were shifted toward the higher values for faster solidification rates. Fraction liquid curve indicates that at the end of melting of the α(Mg)-β(Mg17Al12) eutectic, i.e., 454.2°C the alloy had a 2% liquid phase.
Research limitations/implications: Future research is intended to address the development of a physical simulation methodology representing very high solidification rates used by High Pressure Die Casting (HPDC) and to assess the microstructure refinement as a function of solidification rates.
Practical implications: Advanced simulation capabilities including non-equilibrium thermal and structural characteristics of the magnesium alloys are required for the development of advanced metal casting technologies like vacuum assisted HPDC and its heat treatment.
Originality/value: The presented results point out the direction for future research needed to simulate the alloy solidification in a laboratory environment representing industrial casting processes.
Keywords: AM50 alloy; Thermal analysis; Solidification.

1. Introduction

A scientifically sound understanding of alloy's solidification process and its corresponding structural characteristics is crucial for the development of contemporary light metal casting technologies where non-equilibrium solidification prevails [5,6,15-18]. Advanced laboratory simulation capabilities including controlled melting, solidification and quenching combined with thermal analysis are

required to properly address this issue. Understanding complex metallurgical relations including the effect of the solidification rates on alloy fraction solid evolution, liquidus temperature, etc. is crucial for the development of an adequate data base for computational modeling [5-7].

In the present study a novel laboratory methodology was used to simulate the melting and solidification processes for AM50 magnesium alloy. This approach achieves various microstructure refinement levels for macro size test samples as well as determines solidification rates and the corresponding alloy's thermal characteristics. This concept was used to determine the AM50 magnesium alloy's thermal characteristics during melting and solidification and to evaluate the effect of the solidification rates on the metallurgical reactions and the corresponding microstructures.

2. Experimental procedures

The material used for this study was an AM50 alloy with a chemical composition as follows: Al-5.25%, Mn-0.37%, Si-0.02%, Mg (balance). A cylindrical test sample with a diameter of φ = 16mm and a length of l = 18mm was machined from the ingot. Each sample had a predrilled hole to accommodate a thermocouple positioned at the center of the test sample to collect the thermal data and control the processing temperatures.

The thermal analysis during melting and solidification cycles was carried out using the Universal Metallurgical Simulator and Analyzer (UMSA) [3]. The melting and solidification experiments for the AM50 alloy were carried out using a cover gas. The Argon at 8 bars pressure and a flow rate of up to 50LMP (Liters Per Minute) was used to cool the outside test sample surface to accelerate the solidification process. The thermal analysis signal in the form of heating and cooling curves was recorded during the melting and solidification. The temperature vs. time and the first derivative vs. temperature curves as well as the fraction liquid / fraction solid vs. temperature curves were calculated and plotted. The detail experimental procedure was described in previous papers [4-7].

After completion of the experiments the longitudinal metallographic sections were prepared and light optical microscopy observations together with image analysis were performed to assess the microstructure changes caused by various solidification conditions.

3. Results

The AM50 alloy microstructure consisted of an α(Mg) matrix, a α(Mg)-β($Mg_{17}Al_{12}$) eutectic as well as an Al_8Mn_5 phase [8-12]. Thermal analysis revealed that the melting process of the AM50 alloy started at 433.7±1°C and was completed at 640±1.5°C. Above this temperature the alloy was in a liquid state. Exceeding this temperature increased the alloy's superheat (Figures 1-3). Analysis of the fraction liquid and first derivative curve (Figure 1) provides a good understanding of the phase transformation during the heating cycle as well as the corresponding volume of the liquid phase that evolved during the melting process. Figure 1 indicates that at the end of melting of the α(Mg)-β($Mg_{17}Al_{12}$) eutectic, i.e., 454.2°C (point #2), the alloy had a 2% liquid phase and was most likely located between the magnesium dendrites. Increasing the temperature during the alloy melting process resulted in a gradual increase in the liquid phase that reached 100% volume at 640°C (Figure 1). The thermal analysis heating curve could be used to determine the optimum process parameters for the solution treatment operation (Figures 2 and 3 (#a)). Exceeding 433.7°C during the single step solution treatment would result in incipient melting of the non-equilibrium α(Mg)-β($Mg_{17}Al_{12}$) eutectic phase.

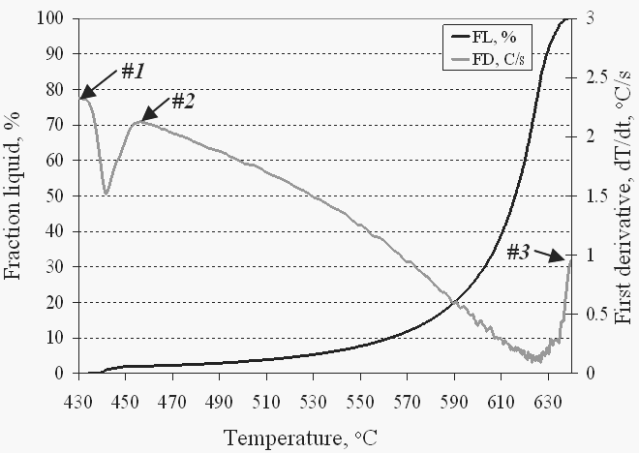

Fig. 1. Temperature vs. fraction liquid (FL) and first derivative (FD) curves recorded during the melting cycle of the AM50 alloy at a 0.8°C/s. The numbers correspond to the various metallurgical reactions

Temperature vs. time cooling curves recorded for the test samples heated to 730°C and solidified at 1°C/s are presented in Figure 2. Two visible temperature arrests were noted on the cooling curves. More detailed information pertaining to the alloy's thermal characteristics such liquidus, nucleation of the α(Mg)-β($Mg_{17}Al_{12}$) eutectic, etc. was collected from the first derivatives curves as on Figure 3 (#b). The temperatures of the metallurgical reactions are pointed out by # numbers. Based on the cooling curve analysis the liquidus temperature was found to be at 625.1°C (Figure 3). At this temperature the first magnesium dendrites, most likely, nucleated from the melt. Latent heat evolved and caused the temperature of the surrounding melt to rise. This point was clearly visible as a sudden change in the first derivative curve (point #4 in Figure 3). With further cooling, the magnesium dendrites continued to grow. At 429.4°C the next change in the first derivative curve was observed and corresponded to the nucleation of the α(Mg)-β($Mg_{17}Al_{12}$) eutectic (Figure 3, point #5). It was found that non-equilibrium solidus temperature was approximately 422.5°C (point #6). Presented thermal characteristics are in good agreement with the reported literature [12-15].

The cooling curves for the AM50 alloy that solidified under a 4°C/s solidification rate are presented in Figures 2 and 3 (#c). It was observed that an instantaneous cooling rate reached up to 9°C/s within the liquid state. The shape of the first derivative curve remained similar as compared with cooling curve of the test

sample that solidified under 1°C/s. It was observed that the beginning of the α(Mg) dendrites' nucleation was shifted up by approximately 10°C, i.e., to 636°C (point #4) as compared with the test sample that solidified under 1°C/s. Similar observations were made for the nucleation temperatures of the α(Mg)-β($Mg_{17}Al_{12}$) eutectic that was shifted up by approximately 10°C, i.e., to 439.7°C (point #5) as compared with the test sample that solidified under a 1°C/s solidification rate. Most likely the reason

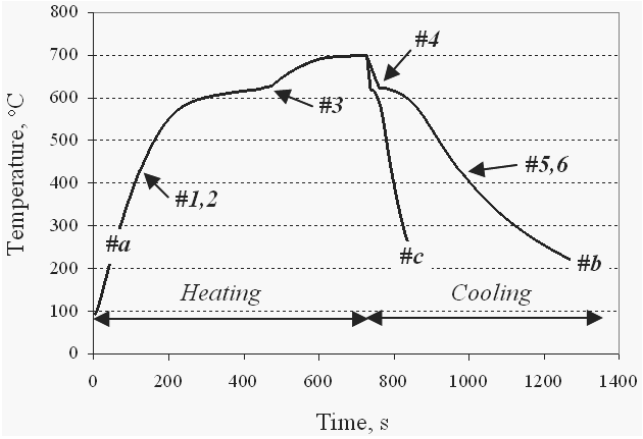

Fig. 2. Temperature vs. time curves of the AM50 alloy test sample recorded during melting at a 0.8◦C/s (#a) and solidification cycles at 1◦C/s (#b) and 4◦C/s (#c). The numbers correspond to the various metallurgical reactions.

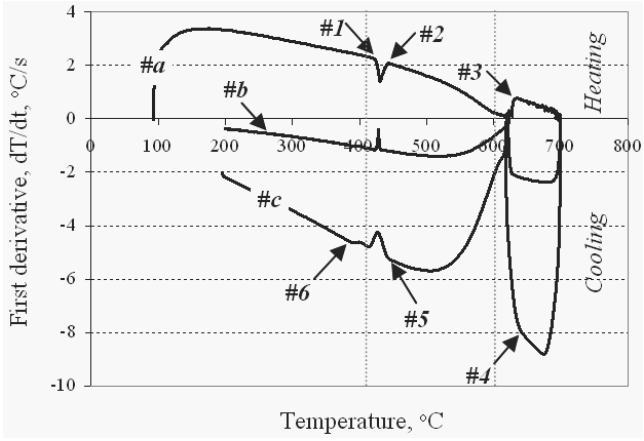

Fig. 3. First derivative (heating/cooling rate) vs. temperature curves of the AM50 alloy test sample recorded during melting at a 0.8◦C/s (#a) and solidification cycles at 1◦C/s (#b) and 4◦C/s (#c). The numbers correspond to the various metallurgical reactions

Metallographic observations of the AM50 test sample solidified at 1°C/s (Figure 4a) revealed the dendritic microstructure of the α(Mg) matrix with visible eutectic regions distributed within the interdenditic spaces. This observation was in agreement with the thermal analysis experiments where two distinct metallurgical reactions were determined on the cooling curve, i.e., nucleation of the α(Mg) dendrites and the α(Mg)-β($Mg_{17}Al_{12}$) eutectic at approximately 625 and 429°C respectively. Image analysis showed that average SDAS was 64.3±12.3μm. Standard deviation represented approximately 20% of the overall SDAS value that was typical for a slowly solidified test sample with a heterogeneous microstructure. Metallographic observations of the AM50 test sample that solidified at a 4°C/s cooling rate revealed significant microstructure refinement caused by the thermal modification mechanism (Figure 4b). The SDAS was reduced to 43.4±9.7μm as compared with 64.3±12.3μm for the test sample that solidified at a 1°C/s cooling rate.

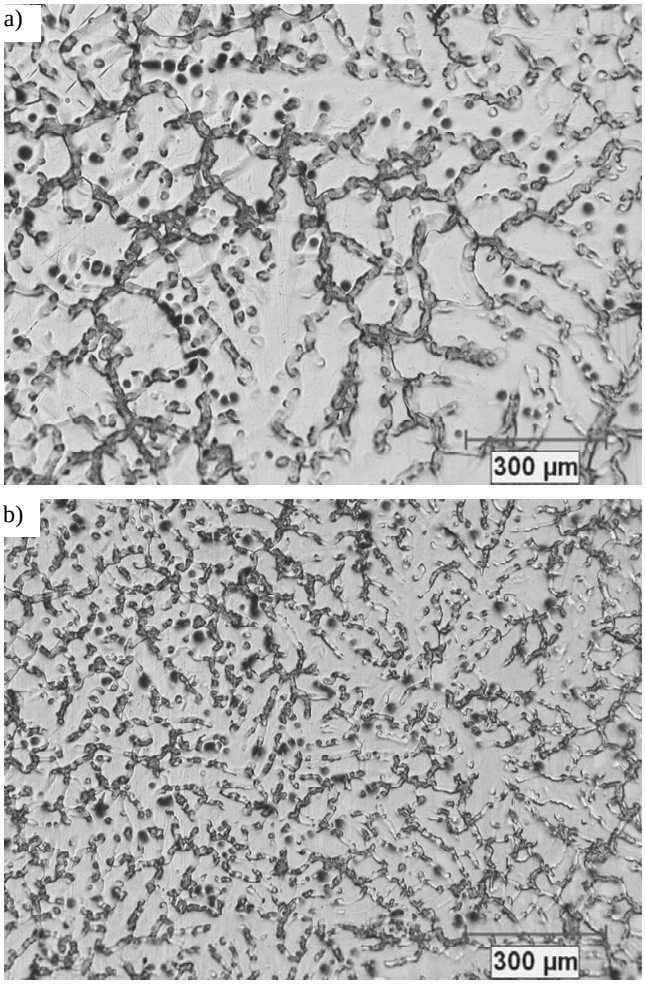

Fig. 4. Optical micrographs (500x) of the AM50 alloy test sample with corresponding SDAS that solidified at the following cooling rates: a) 1°C/s (64.3±12.3μm), b) 4°C/s (43.4±9.7μm)

The SDAS strongly depended on the increased solidification rate that reduced the time necessary for coarsening of the Mg dendrites and that resulted in multiplication of the secondary dendrite arms that distribute the solute content in front of the solidifying interface.

The casting physical simulation methodology outlined in this publication could provide structural and thermal characteristics for rapid solidification experiments with cooling rates exceeding 50°C/s carried out for HPDC optimization studies for hypereutectic Al-Si

alloys [6]. This information could be used for subsequent optimization of the metal casting processing technologies including heat treatment. This data provides valuable input for computer models like the heat transfer coefficient, fraction solid, liquidus, solidus temperatures, etc. obtained for variable solidification rates [7]. Additionally, the effect of thermal or chemical modification (grain refiners, eutectic modifiers, etc.) on selected thermal characteristics like the undercooling temperature can be determined for specific solidification rates representative of specific casting processes (sand, permanent, etc.). Current computer simulation software relies on the thermal characteristics obtained during equilibrium solidification conditions and does not address the effect of the thermal and chemical aspects of microstructure refinement.

4. Conclusions

Based on the solidification experiments and subsequent metallurgical analysis for the AM50 alloy test samples the following was concluded:

- It is feasible for a magnesium macro test sample to achieve a variable solidification rates, the corresponding microstructure refinement and to maintain good resolution of the temperature signal suitable for advanced thermal analysis.
- Generated microstructures are representative of specific sections of the cast component and could be used for subsequent optimization of the post casting processing operations including the heat treatment.
- Thermal analysis performed during solidification experiments at 1 and 4^{o}C/s average cooling rates had satisfactory signal resolution. This allowed for determination of the thermal characteristics and for correlation with alloy microstructure parameters.
- Increasing the solidification rate from 1 to 4^{o}C/s decreased the SDAS of the magnesium matrix from 64.3±12.3μm to 43.4±9.7μm.
- Fraction liquid curve (obtained during the melting) can provide valuable input for determination of the semi-solid processing parameters while fraction solid curves (obtained during the solidification) can determine feeding characteristics of the AM50 alloy.
- Thermal and structural characteristic data could provide valuable input for computer modeling software particularly for non-equilibrium solidification conditions.

Acknowledgements

The authors would like to thank Dr. M. Kasprzak from the Silesian University of Technology in Poland for his valuable contributions to the UMSA Technology Platform's configuration and R. Zavadil from CANMET-MTL for metallographic work. This research is co-funded by AUTO21, a member of the Network of Centres of Excellence of Canada program and within the framework of scientific financial resources of the Ministry of Science and High Education in Poland as a research and development project R15 0702 headed by Prof. L.A. Dobrzański.

References

[1] B.L. Mordike, T. Ebert, Magnesium properties-applications-potentials, Materials Science and Engineering A302 (2001) 37-45.
[2] A. Luo, Magnesium: current and potential automotive applications, JOM 42-48, February, 2002.
[3] J.H. Sokołowski, W.T. Kierkus, M. Kasprzak, W. Kasprzak, Universal Metallurgical Simulator and Analyzer (UMSA) (US Patent No. 7,354,491 B2 April 8, 2008).
[4] W.T. Kierkus, J.H. Sokołowski, Recent advances in CCA: A new method of determining baseline equation, AFS Transactions 14 (1999) 161-167.
[5] H. Yamagata, H. Kurita, M. Aniołek, W. Kasprzak, J.H. Sokołowski, Thermal and metallographic characteristics of the Al-20% Si high-pressure die-casting alloy for monolithic cylinder blocks, Journal of Materials Processing Technology 199 (2007) 84-90.
[6] H. Yamagata, W. Kasprzak, M. Aniołek, H. Kurita, J.H. Sokołowski, The effect of average cooling rates on the microstructure of the Al-20% Si high pressure die casting alloy used for monolithic cylinder blocks, Journal of Materials Processing Technology 204 (2008) 132-140.
[7] H. Onda, K. Sakurai, T. Masuta, K. Oikawa , K. Anzai, W. Kasprzak, J.H. Sokołowski, The effect of solidification models on the prediction results of the temperature change of the aluminum cylinder head estimated by FDM solidification analysis, Trans Tech Publications, Switzerland, Materials Science Forum 561-565 (2007) 1967-1970.
[8] M.M. Avedesian, H. Baker, Magnesium and Magnesium Alloys, ASM International, (1999).
[9] Y. Fasoyinu, P. Newcombe, M. Sahoo, Lost foam casting of magnesium alloys AZ91D and AM50, AFS Transactions 114 (2006) 707-718.
[10] V.Y. Gertsman, J. Li, S. Xu, J.P. Thomson, M. Sahoo, Microstructure and second phase particles in low and high pressure die cast magnesium alloy AM50, Metallurgical and Materials Transactions A 36A 8 (2005) 1989-1997A.
[11] F. Habashi, Alloys-Preparation, Properties, Applications, Wiley-Vch (1998), 151-164.
[12] L. Han, H. Hu, D. Northwood, N. Lie, A calorimetric analysis of dissolution of second phases in as-cast AM50 alloys, Magnesium Technology 12 (2007) 369-373.
[13] D. Mirkovic, R. Schmid-Fetzer, Solidification curves for commercial Mg alloys determined from Differential Scanning Calorimetry with improved heat-transfer modeling, Metallurgical and Materials Transactions A 38A (2007) 2575-2592.
[14] M. Ohno, D. Mirkovic, R. Schmid-Fetzer, Phase equilibria and solidification of Mg-rich Mg-Al-Zn alloys, Materials Science and Engineering A 421 (2006) 328-337.
[15] Y.W. Riddle, L.P. Barber, M.M. Makhlouf, Characterization of Mg solidification and as-cast microstructures, Magnesium Technology 12 (2004) 203-208.
[16] L.A. Dobrzanski, W. Kasprzak, J.H. Sokolowski, Analysis of the Al-Si Alloy structure development using thermal analysis and rapid quenching techniques, Proceedings of the 12th Scientific International Conference "Achievements in Mechanical and Materials Engineering", AMME'2003, Gliwice - Zakopane, 2003, 225-228.
[17] L.A. Dobrzański, T. Tański, L. Čížek, Z. Brytan, Structure and properties of the magnesium casting alloys, Journal of Materials Processing Technology 192-193 (2007) 567-574.
[18] L.A. Dobrzański, T. Tański, J. Trzaska, L. Čížek, Modelling of hardness prediction of magnesium alloys using artificial neural networks applications, Journal of Achievements in Materials and Manufacturing Engineering, 26/2 (2008) 187-190.